Mass and charge flow in nanopores: numerical simulation via mesoscale models

Mauro Chinappi[1], Simone Melchionna[2], Fabio Cecconi[3], Umberto Marini Bettolo Marconi[4], Carlo Massimo Casciola[5]
[1] *Center for Life Nano Science@Sapienza, Istituto Italiano di Tecnologia, Rome, Italy*
E-mail: maurochinappi@gmail.com

[2] *CNR-IPCF, c/o Dipartimento di Fisica, Sapienza Università di Roma, Rome, Italy*
E-mail: simone.melchionna@gmail.com

[3] *CNR-Istituto dei Sistemi Complessi (ISC) UoS "Sapienza", Rome Italy*
E-mail: fabio.cecconi@roma1.infn.it

[4] *Scuola di Scienze e Tecnologie, Università di Camerino, INFN Perugia, Italy*
E-mail: Umberto.Marini.Bettolo@roma1.infn.it

[5] *Dipartimento di Ingegneria Meccanica e Aerospaziale, Sapienza Università di Roma, Italia*
E-mail: carlomassimo.casciola@uniroma1.it

Keywords: Nanofluidics, nanopores, numerical simulations, DNA translocation

SUMMARY. Nanofluidics, thanks to the recent progress in the fabrication of micro and nanodevices, has become an intense research field. Confined fluids in nanoscale geometries exhibit physical behaviors that, in several cases, largely differ from macroscale dynamics. The crucial differences are: i) in nanoscale systems the usual mathematical description for continuum fluid dynamics (Navier-Stokes equation), often fails to reproduce the correct fluid dynamics behavior and ii) in a number of crucial applications the focus is on the motion of a single macromolecule. These occurrences naturally call for an atomistic description of the whole system, which however remains currently limited to relatively small systems (tens of nm simulated for hundreds of ns). The simulation of the fluid motion at nanoscale is here addressed via a recent developed mesoscale approach. In particular the flow of an electrolyte through a nano channel is analyzed. The system represent an experimentally well characterized solid-state nanopore employed for DNA and protein translocation. The simulations are aimed at estimating the effect of DNA translocation on mass and charge flow rate potentially shedding light on the molecular mechanism behind recent experimental observations.

1 INTRODUCTION

Nanopore-based protocols for macromolecule detection and characterization are a promising technology for the development of sensors and devices able to operate at single-molecule level. Their working principle is, in essence, very simple. A nanopore connects two reservoirs containing an electrolyte solution and an applied voltage across the chambers generates a net ion current. When one of the macromolecules dispersed in the solution engages the pore, the ion flux is altered and a change in the current is measured. The intensity, the sign and the duration of the current drop depend on the physico-chemical properties of the passing molecule. Hence the current track can, in principle, provide precise information on a single-molecule level. In the past decade significant efforts have been devoted to nanopore DNA sequencing [1, 2] and recently also proteomic applications have started being explored [3, 4, 5, 6, 7, 8, 9] using both solid-state and biological pores. In this contribution we deal with the mass and charge transport in a solid state nanopore of diameter $D = 6nm$ and length $L = 20nm$. The size is selected in order to resemble the typical size of solid state nanopores that are commonly drilled using FIB or TEM [10, 11] in 20 nm wide silicon nitride (SiN) membranes. In particular we analyze via numerical simulation the effect of a charge distribution at the pore entrance on the mass and charge fluxes across the pore, as a preliminary investigation of the current alteration due to the presence of charged macromolecule, in particular the negatively charged DNA molecule, stuck in front of the pore on the way of translocating.

The contribution is structured as follows: in the section (2) the general electrohydrodynamical model is formulated in term of partial differential equation (Navier-Stokes, Charge transport, Poisson equation) followed by the brief description of the Lattice-Boltzmann (LB) approach used for molecular simulations. In section 3 the preliminary results are presented and discussed.

2 THE MODEL

In this section we discuss the field equations that, under the continuum assumption, properly describe the system, the system geometry and the relevant boundary conditions.

2.1 Field equations

The motion of a dilute electrolyte where only two carrier species are present is described by the following set of partial differential equations for velocity $\mathbf{u}$, pressure p, number density $n^{\pm}$ and electric $\mathbf{E}$ fields defined in the domain $\mathcal{D}$ sketched in Fig. 1:

i) mass conservation

$$\nabla \cdot \mathbf{u} = 0 \tag{1}$$

ii) incompressible Navier-Stokes equation

$$\frac{\partial \mathbf{u}}{\partial t} + \mathbf{u} \cdot \nabla \mathbf{u} = -\frac{1}{\rho}\nabla p - \nu \nabla^2 \mathbf{u} + \frac{\sigma_e}{\rho}\mathbf{E} \tag{2}$$

iii) transport equations for the two charged species

$$\frac{\partial n^{\pm}}{\partial t} + \mathbf{u} \cdot \nabla n^{\pm} = -\nabla \cdot \left[D^{\pm} \nabla n^{\pm} + n^{\pm} \mu^{\pm} e z^{\pm} \mathbf{E}\right] \tag{3}$$

iv) Poisson equation

$$\nabla^2 \Phi = -\frac{\sigma_e}{\epsilon} \tag{4}$$

where, ρ is the fluid density, ν is the kinematic viscosity of the solvent, n^+ and n^- are the number concentrations of the positive and negative charge carriers, respectively, $\sigma_e = e(z^+ n^+ - z^- n^-)$, Φ is the electrical potential such that $\mathbf{E} = -\nabla \Phi$, D^+ and D^- the diffusion coefficient of the carriers and μ^+ and μ^- their nobilities, e the electron charge, $z^{\pm}$ the ion valence, $\epsilon = \epsilon_0 \epsilon_e$, with ϵ_0 the vacuum dielectric constant and ϵ_e the relative permittivity of the solution. The specific assumptions underling the presented model deserve some detailed discussion. As a first comment the description in terms of continuum fields does not take into account the motion of individual molecules. Several studies indicate that for simple fluids this is a good description up to the nanoscale [12, 13, 14]. Since the model is assumed to be valid for dilute solutions, all the fluid properties (ν, ϵ_r, ρ) are taken to be constant (i.e. independent of the charge carrier concentrations) and equal to solvent one (water). In the following, for the sake of simplicity, the electrolytic solution is taken to be symmetric, i.e. the positive and negative carriers have identical valence $z^+ = z^-$ and mobility, i.e. $\mu^+ = \mu^-$.

The model is completed by a prescribed negatively charged distribution of overall intensity Q fixed in front of the pore mouth. This prescribed charge distribution is required to account for the presence of a charged macromolecule, e.g. DNA, stuck in front of the pore prior to translocation. Its presence is expected to alter the currents flowing through the pore by electrostatic interactions. After the present preliminary study, the same tools here introduced will allow to simulate the entire translocation process for a realist model of a DNA molecule [15].

2.2 Boundary condition

In micro and nanofluidic devices in general the proper boundary condition for the tangential component of the velocity $\mathbf{u}$ is the Navier boundary condition that for planar wall reads $V_s = L_s \partial \mathbf{u}_\pi / \partial n$ where $\mathbf{V_s}$ is the fluid velocity relative to the wall, $\mathbf{u}_\pi$ the tangential component of the velocity field, n the direction normal to the wall and L_s the so called slip length[16]. Atomistic simulation and recent experiments suggest that the slip length L_s for water on smooth surfaces hardly exceed $1 - 2nm$[17, 18, 19, 20]. In the system we are interested in, the diameter of the pore is $6nm$. At these scales slip lengths on the order of $1nm$, describing (macroscopically) small deviations from the no-slip boundary condition, can lead to significant modifications in the flow pattern. However, in general, the materials usually employed for fabricating the nanopore are hydrophilic, thus allowing to safely assume the usual no-slip boundary condition.

Concerning the Poisson equation, Gauss law implies the tangential component of $\mathbf{E}$ to be continuous at the liquid-solid interface, i.e. $(\mathbf{E_e})_\pi = (\mathbf{E_w})_\pi$ where the subscript e denotes the electrolyte side and w the solid wall side, and a jump in the normal component

$$\epsilon_0 \epsilon_e \mathbf{E_e} \cdot \hat{\mathbf{n}} = \epsilon_0 \epsilon_w \mathbf{E_w} \cdot \hat{\mathbf{n}} + q_w \ , \tag{5}$$

where q_w is the surface charge distribution at the interface. In practical cases the huge disparity in the dielectric constants, $\epsilon_e \simeq 80$ for liquid water and $\epsilon_w \sim 5$ ($\epsilon_w \simeq 3.9$ for silicon oxide and $\epsilon_w \simeq 7.9$ for silicon nitride) for the wall, allows to simplify Eq. (5) in the form

$$\frac{\partial \Phi}{\partial n} = -\frac{q_w}{\epsilon_0 \epsilon_e} \ . \tag{6}$$

Fully developed flow is assumed at the inlet (blue, in Fig.1) and outlet (red) sections, modeled as electrodes at prescribed electrical potential ($\phi_{in} = 0$ and $\phi_{out} = \Delta V$). Dirichlet boundary conditions enforce the bulk concentration n_{bulk} of the two charged species at inlet and outlet, namely $n^+_{in} = n^+_{out} = n^-_{in} = n^-_{out}$.

2.3 *Numerical approach*

The dynamics described by the system of equation (1-4) is simulated by a version of the so-called Lattice Boltzmann Method [21, 15], a computational technique inspired to the classical Boltzmann

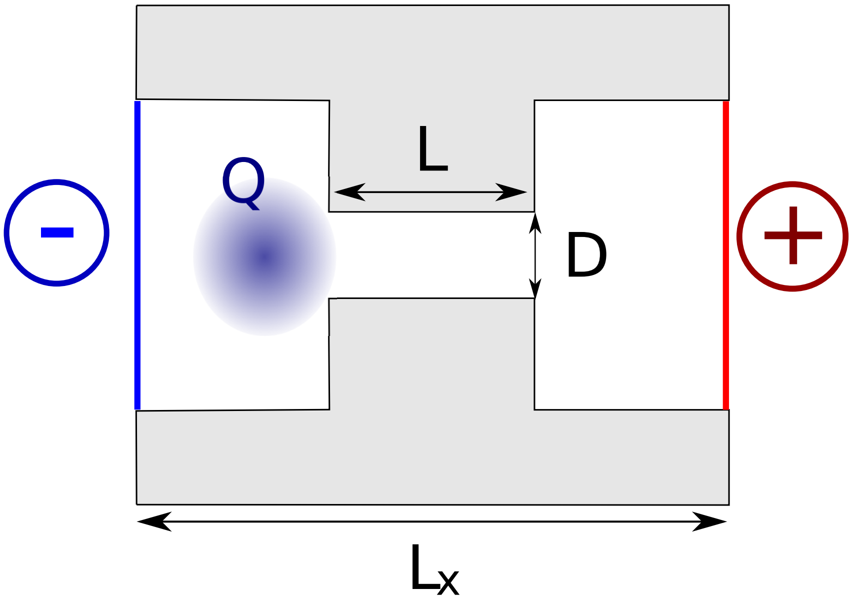

Figure 1: System set-up. The cylindrical nanopore (diameter D, length L) connects two reservoirs (diameter $3D$, length L each). A voltage is applied between inlet and outlet (blue –negative– and red –positive– lines). The negative charge distribution Q is positioned at the pore entrance.

equation for the evolution of a particle population. The macroscopic fields are recovered by properly averaging the particle microscopic distribution. Space is discretized in a cubic mesh of size a and the continuous distribution of microscopic velocity is restricted to a set of 19 values, describing the streaming from one cell to one of its 6 first neighbors and 12 second neighbors completed by the null velocity state for particles at rest. A collision step accounts for determining the microscopic velocity. In the present case [22, 23, 24], three different particle populations are evolved corresponding to the neutral solvent and the two charged species. In addition a Poisson solver is used for the electric field. The prescribed charge distribution stuck in front of the pore is discretized as a system of regularized point-wise charges. From the three distributions one can extract information on the resulting macroscopic fields, e.g. overall solution velocity $\mathbf{u}$ or the velocity of each single species, $\mathbf{u}^0$, $\mathbf{u}^+$, and $\mathbf{u}^-$.

3 NUMERICAL RESULTS

Before presenting the data we briefly report the units of measurement employed. Lengths are measured in units of lattice spacing. Time is measured in units of the discrete step of the lattice Boltzmann solver. Electron charge e is assumed to be unitary as well as the bulk fluid density ρ. The thermal energy k_BT is specified by fixing the thermal velocity whose value is $v_T = (k_BT/m)^{1/2} = 1/3^{1/2}$ in lattice units [22]. The dielectric constant is imposed via the Bjerrum length, $l_B = e^2/(4\pi\epsilon k_BT)$. In order to map the code units in actual ones, as a first step it is needed to set the lattice length, in our case for instance one lattice length corresponds to $0.2nm$. Then mapping the fluid viscosity it is possible to express the value of the lattice Boltzmann solver time unit in seconds. Values of electron charge and liquid mass density allow to convert all the other quanti-

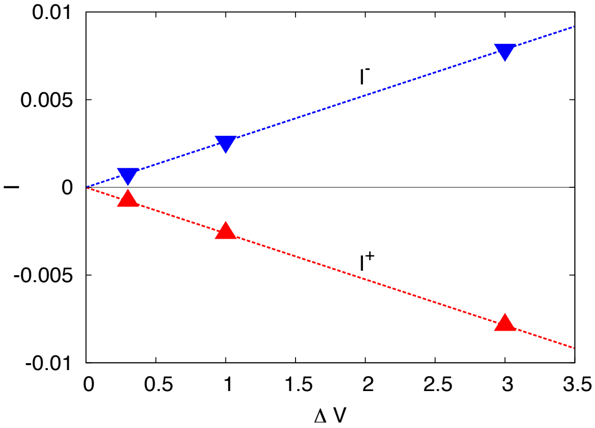

Figure 2: Currents as a function of the applied voltage ΔV for $Q = 0$. It is apparent that the positive and negative carries contribute to the correct equally, i.e. their current are equal in magnitude and opposite in sign.

ties such as potential drop and electric field. For the purpose of the present preliminary study it is not needed to map the results in actual units, hence in the following data are reported in the above defined lattice units.

The observables we focus on are the mass fluxes defined as

$$M^\alpha = \frac{1}{L}\int u_x^\alpha \rho^\alpha dV\,, \tag{7}$$

where $\alpha = +, -, 0$ refers to the species considered and the mass density is simply $\rho^\alpha = n^\alpha m^\alpha$ where m^α is the mass of the single molecule of each species. The total mass flux is $M = M^0 + M^+ + M^-$. The resulting electric current I can be expressed as the sum of the partial electric currents, $I = |I^+ - I^-|$, where $I^\pm = e(z^\pm M^\pm/m^\pm)$ where e is the electron charge here assumed equal to unity. Here we assume $z^\pm = 1$.

As a first step in our analysis we verify the behavior of our observables in absence of the prescribed charge Q. Fig. 2 reports I^+ and I^- as a function of the applied voltage ΔV. It is apparent that the two currents, I^+ and I^-, have the same intensity and opposite signs (towards the negative electrode for $+$, towards the positive one for $-$, implying that the electric currents have the same direction once the sign of the transported charge is included). This is expected in a system where the two charge carriers are symmetric (same bulk concentration, same mobilities, same ion valence). The solvent is at rest, e.g. $M^0 = 0$, since locally, the forces exerted by the two opposed charged species on the neutral one mutually cancel out, due to the symmetry of the electrolyte. The currents $I^\pm$ appear to be proportional to the applied potential, implying that the usual Ohm's law for electric current holds in the voltage range explored.

The effect on the currents of the presence of the static negative charge Q in front of the pore mouth, see the sketch in Fig. 1, is summarized in Fig. 3 for several simulations at changing the intensity of the charge Q and constant applied voltage. In panel the left panel of the figure the currents $I^\pm$ are plotted as function of the charge intensity. The quantities reported in the figure are the absolute values of the currents, since I^+ concerns the positively charged species which moves

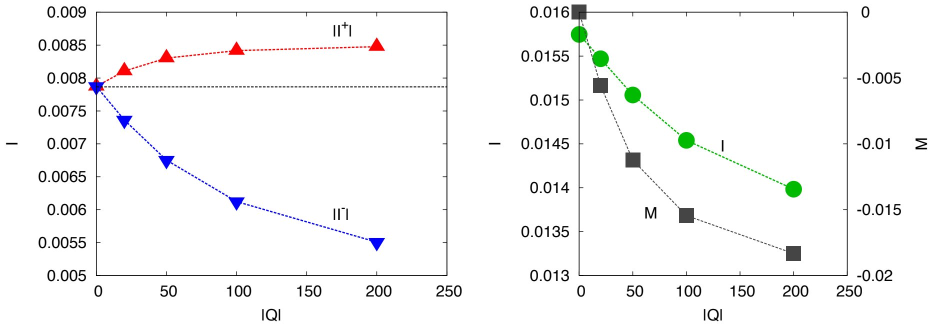

Figure 3: Left) Current I as a function of the absolute value of the (negative) charge Q for $\Delta V = 3$. Right. Total electrical current I and mass flow rate M.

in the negative x-direction, from the positive to the negative electrode (i.e. $I^+ \leq 0$). Analogously $I^- \geq 0$. As already discussed, at $Q = 0$ the two current intensities are identical, see also Fig. 2. The presence of an increasingly negative charge Q induces the increase of the local number density of positive charge carriers. Consistently $|I^+|$ increases, while at the same time $|I^-|$ decreases. The decrease of $|I^-|$ is however larger than the increase in $|I^+|$, resulting in the monotone decrease of the resulting electric current $I = |I^+ - I^-|$, see the green circles in the right panel of the figure. The unbalance between the mass fluxes of the two charge carriers induces a net force on the neutral species. As a consequence an overall electro-osmotic flux, dominated by the neutral, abundant species, is generated. The fluid streams in the direction of the mass flux of the positive charge carriers towards the negative electrode (i.e. the mass flux is negative, see the scale on the second ordinate axis on the right of the plot). Fig. 4 reports the concentration and the flux of positive and negative carriers for $Q = -100$. It is apparent that the present of the charge alters the carrier distribution.

4 CONCLUSIONS

The present study provided evidence of the substantial effect a negative charge stationary at the pore mouth may have on the mass and charge transport through a nanopore subject to a voltage. Interestingly the resulting electric current is found to decrease as a function of the charge strength $|Q|$. The unbalance between the mass flux of the two oppositely charge carriers gives rise to a net electro-osmotic flux, driven by the dominating mass flux of the positive free charges. These preliminary results open the way to the application of the proposed meso-scale approach to simulate and interpret the experimentally observed current signature associated to the interaction of a neatly charged bio-molecule (e.g. DNA) and solid state nanopores.

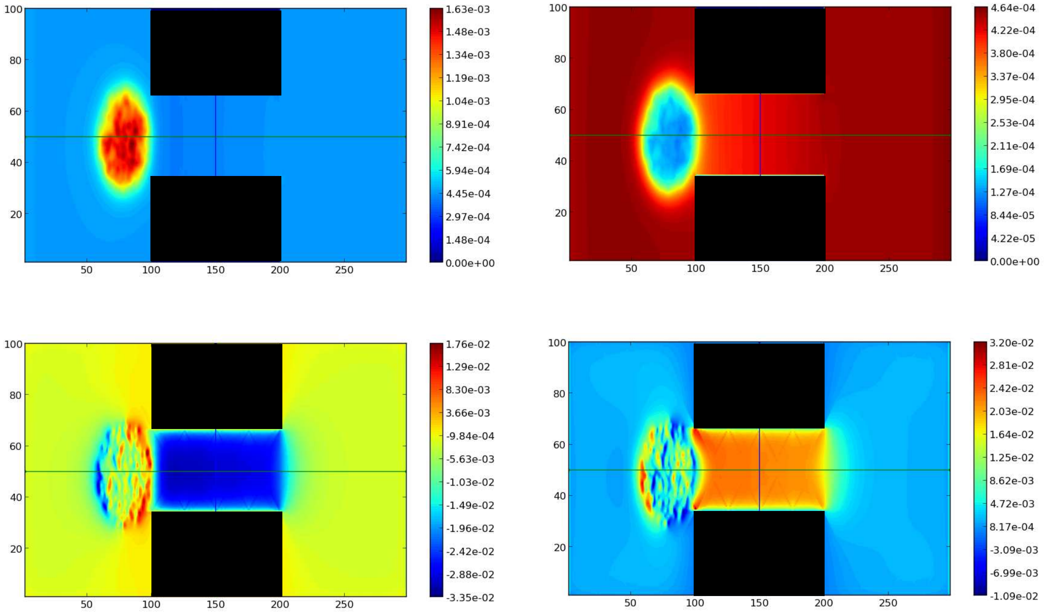

Figure 4: Upper panels: n^+ (left) and n^- (right) fields. It is apparent that the presence of the negative charge outside the pore, alters the carrier distributions. In particular n^+ in the pore is larger than the bulk value while the opposite happens for n^-. Lower panels: $x-$component of the flux of n^+ (left) and n^- specie.

References

[1] G.F. Schneider and C. Dekker. Dna sequencing with nanopores. *Nature biotechnology*, 30(4):326–328, 2012.

[2] E. Pennisi. Search for pore-fection. *Science*, 336(6081):534–537, 2012.

[3] D. Rotem, L. Jayasinghe, M. Salichou, and H. Bayley. Protein detection by nanopores equipped with aptamers. *Journal of the American Chemical Society*, 134(5):2781–2787, 2012.

[4] A.G. Oukhaled, A.L. Biance, J. Pelta, L. Auvray, and L. Bacri. Transport of long neutral polymers in the semidilute regime through a protein nanopore. *Physical Review Letters*, 108(8):88104, 2012.

[5] C. Madampage, O. Tavassoly, C. Christensen, M. Kumari, and J.S. Lee. Nanopore analysis: An emerging technique for studying the folding and misfolding of proteins. *Prion*, 6(2):110–118, 2012.

[6] D.S. Talaga and J. Li. Single-molecule protein unfolding in solid state nanopores. *Journal of the American Chemical Society*, 131(26):9287–9297, 2009.

[7] M.M. Mohammad, R. Iyer, K.R. Howard, M.P. McPike, P.N. Borer, and L. Movileanu. Engineering a rigid protein tunnel for biomolecular detection. *Journal of the American Chemical Society*, 134(22):9521–9531, 2012.

[8] M. Bacci, M. Chinappi, C.M. Casciola, and F. Cecconi. Role of denaturation in maltose binding protein translocation dynamics. *The Journal of Physical Chemistry B*, 116(14):4255–4262, 2012.

[9] M. Chinappi, F. Cecconi, and C. M. Casciola. Computational analysis of maltose binding protein translocation. *Philos. Mag.*, 91(13-15):2034–2048, 2011.

[10] Stefan W Kowalczyk, Adam R Hall, and Cees Dekker. Detection of local protein structures along dna using solid-state nanopores. *Nano letters*, 10(1):324–328, 2009.

[11] Stefan W Kowalczyk and Cees Dekker. Measurement of the docking time of a dna molecule onto a solid-state nanopore. *Nano letters*, 12(8):4159–4163, 2012.

[12] M. Chinappi, S. Melchionna, C.M. Casiola, and S. Succi. Mass flux through asymmetric nanopores: microscopic versus hydrodynamic motion. *The Journal of Chemical Physics*, 129:124717, 2008.

[13] Mauro Chinappi. Applications of all-atom molecular dynamics to nanofluidics.

[14] Lydéric Bocquet and Elisabeth Charlaix. Nanofluidics, from bulk to interfaces. *Chemical Society Reviews*, 39(3):1073–1095, 2010.

[15] Massimo Bernaschi, Simone Melchionna, Sauro Succi, Maria Fyta, Efthimios Kaxiras, and Joy K Sircar. Muphy: A parallel multi physics/scale code for high performance bio-fluidic simulations. *Computer Physics Communications*, 180(9):1495–1502, 2009.

[16] L. Bocquet and J.L. Barrat. Flow boundary conditions from nano- to micro-scales. *Soft Matter*, 3(6):685–693, 2007.

[17] M. Chinappi and CM Casciola. Intrinsic slip on hydrophobic self-assembled monolayer coatings. *Physics of Fluids*, 22:042003, 2010.

[18] D. Gentili, M. Chinappi, G. Bolognesi, A. Giacomello, and C.M. Casciola. Water slippage on hydrophobic nanostructured surfaces: molecular dynamics results for different lling levels. *Meccanica*, page In print, 2013.

[19] L. Huang and D.E. Makarov. Translocation of a knotted polypeptide through a pore. *The Journal of Chemical Physics*, 129:121107, 2008.

[20] Phil Attard. More reliable measurements of the slip length with the atomic force microscope. *arXiv preprint arXiv:1302.6630*, 2013.

[21] Shiyi Chen and Gary D Doolen. Lattice boltzmann method for fluid flows. *Annual review of fluid mechanics*, 30(1):329–364, 1998.

[22] Umberto Marini Bettolo Marconi and Simone Melchionna. Charge transport in nanochannels: a molecular theory. *Langmuir*, 28(38):13727–13740, 2012.

[23] Umberto Marini Bettolo Marconi, Simone Melchionna, and Ignacio Pagonabarraga. Effective electrodiffusion equation for non-uniform nanochannels. *The Journal of Chemical Physics*, 138:244107, 2013.

[24] Simone Melchionna and U Marini Bettolo Marconi. Electro-osmotic flows under nanoconfinement: A self-consistent approach. *EPL (Europhysics Letters)*, 95(4):44002, 2011.